Available online at www.sciencedirect.com
SCIENCE DIRECT®
Journal of Sound and Vibration 280 (2005) 63–76
JOURNAL OF SOUND AND VIBRATION
www.elsevier.com/locate/jsvi

Modal analysis of constrained multibody systems undergoing rotational motion

Dong Hwan Choi[a], Jung Hun Park[b], Hong Hee Yoo[a,*]

[a] *School of Mechanical Engineering, Hanyang University, Sungdong-Gu Haengdang-Dong 17, Seoul 133-791, South Korea*

[b] *Mechatronics Center, Samsung Electronics Co., Ltd, 416 Maetan-3Dong, Paldal-Gu, Suwon, Kyungki-Do 442-742, South Korea*

Received 9 June 2003; accepted 1 December 2003

Abstract

The modal characteristics of constrained multibody systems undergoing rotational motion are investigated in this paper. Relative co-ordinates are employed to derive the equations of motion, which are generally non-linear in terms of the co-ordinates. The dynamic equilibrium position of a constrained multibody system needs to be obtained from the non-linear equations of motion, which are then linearized at the dynamic equilibrium position. The mass and the stiffness matrices for the modal analysis can be obtained from the linearized equations of motion. To verify the effectiveness and the accuracy of the proposed method, numerical examples are solved and the results obtained by using the proposed method are compared with analytical and numerical results obtained by other methods. The proposed method can be used effectively for the design of constrained multibody systems undergoing rotational motion.

1. Introduction

Mechanical systems can be modelled as constrained multibody systems that consist of rigid and flexible bodies, joints, springs, dampers, forces and so on. In general, the equations of motion governing constrained multibody systems consist of non-linear differential and algebraic equations. To obtain the response of a constrained multibody system, several computational methods were introduced since early 1960s (see Refs. [1–4]). Several commercial programs for multibody system analysis (see, for instance, Refs. [5–7]) are available nowadays. By using these

*Corresponding author. Fax: +82-2-2293-5070.
E-mail addresses: esprit@ihanyang.ac.kr (D.H. Choi), hynpjh@mail.metric.or.kr (Jung Hun Park), hhyoo@hanyang.ac.kr (Hong Hee Yoo).

0022-460X/$ - see front matter © 2003 Elsevier Ltd. All rights reserved.
doi:10.1016/j.jsv.2003.12.011

programs, kinematic, dynamic, and static equilibrium analyses of constrained multibody systems can be performed. If a constrained multibody system has a static equilibrium position (this is often called a state of rest), its modal characteristics, which are often important for system design, can be also obtained. Equations of motion are linearized at the static equilibrium position and the mass and the stiffness matrices for the modal analysis can be obtained. Sohoni and Whitesell [8] introduced a linearization method based on a generalized co-ordinate partitioning method in which dependent co-ordinates are eliminated. Lynch and Vanderploeg [9] proposed another linearization method employing QR decomposition by which a constrained set of equations can be converted to an unconstrained set of equations. By using these methods, the modal characteristics of a constrained multibody system in state of rest could be obtained.

There exists a state of motion which resembles the state of rest. In the state of motion, one may choose a set of generalized co-ordinates which becomes constant. This state which is determined by the set of generalized co-ordinates will be hereinafter called a dynamic equilibrium state. For explanation, let us consider a rotating pendulum system shown in Fig. 1. The pendulum is connected by a revolute joint and the vertical shaft is made to rotate with a constant angular speed. The dynamic equilibrium state of the system can be easily calculated if a proper generalized co-ordinate is chosen. The angle between the shaft and the pendulum may be chosen as the generalized co-ordinate, which becomes constant at the dynamic equilibrium state. It is important to choose a proper set of generalized co-ordinates if one has the purpose to find the dynamic equilibrium state effectively. As shown from the above example, relative angles and displacements between bodies are the best candidates for the purpose. Such co-ordinates are often called relative co-ordinates (see, for instance, Refs. [10,11]).

Constrained multibody systems undergoing rotational motion (such as rotating pendulums) exhibit distinct modal characteristics. As their angular speeds vary, their natural frequencies usually vary, too. The varying modal characteristics need to be predicted accurately for a proper system design. However, the varying modal characteristics cannot be calculated directly by using any existing multibody analysis programs (though some of them have the capability to calculate the modal characteristics of constrained multibody systems in states of rest). Actually, even dynamic equilibrium states cannot be calculated efficiently by using any existing commercial codes. To obtain a dynamic equilibrium state of a constrained multibody system (by using existing

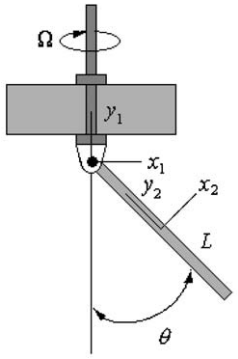

Fig. 1. Configuration of a rotating pendulum system.

commercial codes), a transient dynamic analysis should be performed with a prescribed rotational motion, which increases smoothly and reaches constant angular velocity. Then the modal characteristics can be obtained by analyzing the oscillatory motion around the dynamic equilibrium state. If the system has one degree of freedom, one may count the number of oscillation to find the natural frequency. However, if the system has more than one degree of freedom, the oscillatory motion has to be analyzed by using a Fourier transformation method. This procedure is time consuming and obviously not proper for design.

The purpose of this paper is to propose a numerical method to calculate the modal characteristics of constrained multibody systems undergoing rotational motion. Relative co-ordinates are employed to describe a constrained multibody system and a velocity transformation matrix is employed to derive the equations of motion. If the system has closed kinematic loops, constraint forces arising from the closed-loops can be eliminated by using the velocity transformation matrix. A formulation to seek the dynamic equilibrium state of a constrained multibody system undergoing rotational motion is first presented. Then linearization procedures for open and closed-loop systems are presented. To verify the effectiveness and the accuracy of the proposed method, numerical examples are solved and the results are compared with analytical and numerical solutions by other methods.

2. Equations of motion

In three-dimensional space, a free rigid body's configuration can be determined by six co-ordinates. Three scalar variables are employed to determine the position of a point (for instance, the center of mass) fixed in the rigid body and three successive rotation angles (often named as Euler angles) are employed to determine the orientation of the body. The co-ordinate set of the ith body of a multibody system is denoted as $\mathbf{x}_i$. If a multibody system consists of n rigid bodies, its total co-ordinate set (named and denoted as a Cartesian co-ordinate set $\mathbf{x}$) consists of n co-ordinate sets as follows:

$$\mathbf{x} = [\mathbf{x}_1^{\mathrm{T}} \quad \mathbf{x}_2^{\mathrm{T}} \quad \cdots \quad \mathbf{x}_n^{\mathrm{T}}]^{\mathrm{T}}. \tag{1}$$

By employing the Cartesian co-ordinate set, the equations of motion of a constrained multibody system can be derived (see Ref. [12]) as follows:

$$\mathbf{M}\ddot{\mathbf{x}} + \boldsymbol{\Phi}_{\mathbf{x}}^{\mathrm{T}}\boldsymbol{\lambda} = \mathbf{Q}, \tag{2}$$

where $\mathbf{M}$ is a mass matrix, $\mathbf{Q}$ is a generalized force matrix, and $\boldsymbol{\lambda}$ is a Lagrange multiplier matrix. The matrix $\boldsymbol{\Phi}$ represents algebraic constraint equations that originate from kinematic joints and $\boldsymbol{\Phi}_{\mathbf{x}}$ is the Jacobian matrix which is the partial derivative of the constraint equations with respect to the Cartesian co-ordinate set.

A closed-loop multibody system can be transformed into a open-loop multibody system by cutting joints as shown in Fig. 2. So, the number of cut joints is same as the number of closed loops. The constraint equations that originate from the cut joints are denoted as $\boldsymbol{\Phi}^c$ and the rest of the constraint equations are denoted as $\boldsymbol{\Phi}^r$. So, the total constraint equations consist of the two sets of equations as follows:

$$\boldsymbol{\Phi} = [\boldsymbol{\Phi}^{c^{\mathrm{T}}} \quad \boldsymbol{\Phi}^{r^{\mathrm{T}}}]^{\mathrm{T}}. \tag{3}$$

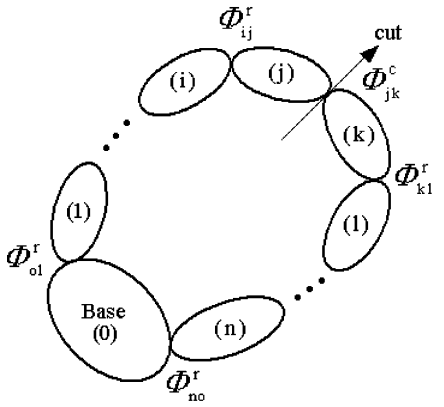

Fig. 2. Schematic representation of a closed-loop system.

Now Eq. (2) can be rewritten as follows:

$$\mathbf{M}\ddot{\mathbf{x}} + \mathbf{\Phi}_{\mathbf{x}}^{c\mathrm{T}}\boldsymbol{\lambda}^c + \mathbf{\Phi}_{\mathbf{x}}^{r\mathrm{T}}\boldsymbol{\lambda}^r = \mathbf{Q}, \tag{4}$$

where $\boldsymbol{\lambda}^c$ and $\boldsymbol{\lambda}^r$ represent the Lagrange multipliers for $\mathbf{\Phi}^c_{\mathbf{x}}$ and $\mathbf{\Phi}^r_{\mathbf{x}}$, respectively.

The equations of motion can be transformed into a reduced form by employing relative co-ordinates. For the purpose, the following relation is often employed:

$$\dot{\mathbf{x}} = \mathbf{B}\dot{\mathbf{q}}, \tag{5}$$

where $\mathbf{B}$ is the velocity transformation matrix, $\dot{\mathbf{q}}$ is the time derivative of relative co-ordinates $\mathbf{q}$ and the transpose of $\mathbf{B}$ is the null space of $\mathbf{\Phi}_{\mathbf{x}}^{r\mathrm{T}}$. This relation is often called the velocity transformation (see, Ref. [13]). One may choose some of $\dot{\mathbf{q}}$ (which will be denoted as $\dot{\mathbf{q}}_P$) to prescribe a constant rotational motion for a constrained multibody system. The rest of $\dot{\mathbf{q}}$ will be denoted as $\dot{\mathbf{q}}_R$. Then, Eq. (5) can be rewritten as follows:

$$\dot{\mathbf{x}} = \mathbf{B}_P\dot{\mathbf{q}}_P + \mathbf{B}_R\dot{\mathbf{q}}_R, \tag{6}$$

where the velocity transformation matrix $\mathbf{B}_P$ and $\mathbf{B}_R$ are sub-matrices associated with the co-ordinates $\mathbf{q}_P$ and $\mathbf{q}_R$.

Now, by differentiating Eq. (6), the following equations can be obtained:

$$\ddot{\mathbf{x}} = \mathbf{B}_P\ddot{\mathbf{q}}_P + \dot{\mathbf{B}}_P\dot{\mathbf{q}}_P + \mathbf{B}_R\ddot{\mathbf{q}}_R + \dot{\mathbf{B}}_R\dot{\mathbf{q}}_R. \tag{7}$$

Now substituting Eq. (7) into Eq. (4) and pre-multiplying the results by $\mathbf{B}_R^{\mathrm{T}}$, one obtains the following equation:

$$\mathbf{B}_R^{\mathrm{T}}[\mathbf{M}(\dot{\mathbf{B}}_P\dot{\mathbf{q}}_P + \mathbf{B}_R\ddot{\mathbf{q}}_R + \dot{\mathbf{B}}_R\dot{\mathbf{q}}_R) + \mathbf{\Phi}_{\mathbf{x}}^{c\mathrm{T}}\boldsymbol{\lambda}^c] = \mathbf{B}_R^{\mathrm{T}}\mathbf{Q}. \tag{8}$$

Note that $\mathbf{B}_R^{\mathrm{T}}\mathbf{\Phi}_{\mathbf{x}}^{r\mathrm{T}}$ and $\ddot{\mathbf{q}}_P$ are null matrices (since $\mathbf{B}^{\mathrm{T}}$ is the null space of $\mathbf{\Phi}_{\mathbf{x}}^{r\mathrm{T}}$ and $\dot{\mathbf{q}}_P$ is constant). Now the following relation can be used to further simplify the above equation:

$$\mathbf{\Phi}_{\mathbf{q}_R} = \frac{\partial\mathbf{\Phi}}{\partial\mathbf{x}}\frac{\partial\mathbf{x}}{\partial\mathbf{q}_R} = \mathbf{\Phi}_{\mathbf{x}}\frac{\partial\dot{\mathbf{x}}}{\partial\dot{\mathbf{q}}_R} = \mathbf{\Phi}_{\mathbf{x}}\mathbf{B}_R, \tag{9}$$

where the dot cancellation law (see Ref. [14]) is employed. By using Eq. (9), Eq. (8) can be rewritten as follows:

$$\mathbf{M}^*\ddot{\mathbf{q}}_R + \mathbf{\Phi}^{c\mathrm{T}}_{\mathbf{q}_R}\boldsymbol{\lambda}^c = \mathbf{Q}^*, \tag{10}$$

where

$$\mathbf{M}^* = \mathbf{B}_R^{\mathrm{T}}\mathbf{M}\mathbf{B}_R, \tag{11}$$

$$\mathbf{Q}^* = \mathbf{B}_R^{\mathrm{T}}\mathbf{Q} - \mathbf{B}_R^{\mathrm{T}}(\mathbf{M}\dot{\mathbf{B}}_P\dot{\mathbf{q}}_P + \mathbf{M}\dot{\mathbf{B}}_R\dot{\mathbf{q}}_R). \tag{12}$$

The acceleration constraint equations, the second time derivatives of the constraint equations $\mathbf{\Phi}^c = 0$, can be written as follows:

$$\mathbf{\Phi}^c_{\mathbf{q}_R}\ddot{\mathbf{q}}_R = \boldsymbol{\gamma}^c, \tag{13}$$

where

$$\boldsymbol{\gamma}^c = -(\mathbf{\Phi}^c_{\mathbf{q}_R}\dot{\mathbf{q}}_R)_{\mathbf{q}_R}\dot{\mathbf{q}}_R - 2\mathbf{\Phi}^c_{\mathbf{q}_R t}\dot{\mathbf{q}}_R - \mathbf{\Phi}^c_{tt}. \tag{14}$$

Eqs. (10) and (13) are used to perform a dynamic analysis of a constrained multibody system undergoing a constant rotational motion.

3. Linearization and modal equations

In order to find the modal characteristics of a constrained multibody system undergoing constant rotational motion, the dynamic equilibrium state of the system has to be found first. Since relative co-ordinates are employed, $\mathbf{q}_R$ becomes constant at the dynamic equilibrium state. So its time derivatives $\dot{\mathbf{q}}_R$ and $\ddot{\mathbf{q}}_R$ are all zero. Substituting these conditions into Eq. (10), one can obtain the following algebraic equations to find the equilibrium state:

$$\mathbf{B}_R^{\mathrm{T}}(\mathbf{M}\dot{\mathbf{B}}_P\dot{\mathbf{q}}_P - \mathbf{Q}) + \mathbf{\Phi}^{c\mathrm{T}}_{\mathbf{q}_R}\boldsymbol{\lambda}^c = 0. \tag{15}$$

The above equations along with the constraint equations ($\mathbf{\Phi}^c = 0$) have to be solved to find the dynamic equilibrium positions. Since these equations are non-linear, the well-known Newton–Raphson procedure can be used to solve them. The detailed procedure is given as follows:

$$\mathbf{f}_{\mathbf{z}}\Delta\mathbf{z}^i = -\mathbf{f}, \tag{16}$$

$$\mathbf{z}^{i+1} = \mathbf{z}^i + \Delta\mathbf{z}^i, \tag{17}$$

where

$$\mathbf{f} = \begin{bmatrix} \mathbf{B}_R^{\mathrm{T}}(\mathbf{M}\dot{\mathbf{B}}_P\dot{\mathbf{q}}_P - \mathbf{Q}) + \mathbf{\Phi}^{c\mathrm{T}}_{\mathbf{q}_R}\boldsymbol{\lambda}^c \\ \mathbf{\Phi}^c \end{bmatrix}, \tag{18}$$

$$\mathbf{z} = \begin{bmatrix} \mathbf{q}_R \\ \boldsymbol{\lambda}^c \end{bmatrix}. \tag{19}$$

By solving the above equations, $\mathbf{q}_R$ and $\boldsymbol{\lambda}^c$ can be obtained. The values of $\mathbf{q}_R$ which are obtained from the equilibrium equations will be used later to obtain the modal equations.

To obtain the modal equations, Eq. (10) has to be transformed into a minimum set of equations of motion. For the purpose, the generalized co-ordinate partitioning method is employed and $\mathbf{q}_R$ is partitioned as follows:

$$\mathbf{q}_R = [\mathbf{u}^{\mathrm{T}} \quad \mathbf{v}^{\mathrm{T}}]^{\mathrm{T}}, \tag{20}$$

where $\mathbf{u}$ and $\mathbf{v}$ represent dependent and independent co-ordinate sets, respectively. Several methods of selecting independent co-ordinate sets are known (see, for instance, Ref. [12]). Differentiation of the constraint equations ($\mathbf{\Phi}^c = 0$) yields the following constraint velocity equations:

$$\mathbf{\Phi}^c_{\mathbf{q}_R}\dot{\mathbf{q}}_R = 0. \tag{21}$$

This equations can be rewritten in terms of dependent and independent velocity vectors $\dot{\mathbf{u}}$ and $\dot{\mathbf{v}}$ as

$$\mathbf{\Phi}^c_{\mathbf{u}}\dot{\mathbf{u}} + \mathbf{\Phi}^c_{\mathbf{v}}\dot{\mathbf{v}} = 0. \tag{22}$$

Therefore, the constraint Jacobian matrix $\mathbf{\Phi}^c_{\mathbf{q}_R}$ should be partitioned as follows:

$$\mathbf{\Phi}^c_{\mathbf{q}_R} = [\mathbf{\Phi}^c_{\mathbf{u}} \quad \mathbf{\Phi}^c_{\mathbf{v}}], \tag{23}$$

where the Jacobian matrices $\mathbf{\Phi}^c_{\mathbf{u}}$ and $\mathbf{\Phi}^c_{\mathbf{v}}$ are sub-Jacobian matrices associated with the co-ordinates $\mathbf{u}$ and $\mathbf{v}$.

Now, $\dot{\mathbf{q}}_R$ can be expressed as a function of $\dot{\mathbf{v}}$ as follows:

$$\dot{\mathbf{q}}_R = \mathbf{R}\dot{\mathbf{v}}, \tag{24}$$

where $\mathbf{R}$ is defined as follows:

$$\mathbf{R} = \begin{bmatrix} -\mathbf{\Phi}^{c-1}_{\mathbf{u}}\mathbf{\Phi}^c_{\mathbf{v}} \\ \mathbf{I} \end{bmatrix}. \tag{25}$$

Pre-multiplying Eq. (10) by $\mathbf{R}^{\mathrm{T}}$ results in a minimum set of equations of motion as follows:

$$\mathbf{R}^{\mathrm{T}}\mathbf{M}^*\mathbf{R}\ddot{\mathbf{v}} + \mathbf{R}^{\mathrm{T}}\mathbf{M}^*\dot{\mathbf{R}}\dot{\mathbf{v}} - \mathbf{R}^{\mathrm{T}}\mathbf{Q}^* = 0. \tag{26}$$

Note that $\mathbf{R}^{\mathrm{T}}$ is the null space of $\mathbf{\Phi}^{c\mathrm{T}}_{\mathbf{q}_R}$. Eq. (26) can be linearized at the dynamic equilibrium state and the following modal equations can be obtained to investigate the modal characteristics of the system:

$$\hat{\mathbf{M}}^*\delta\ddot{\mathbf{v}} + \hat{\mathbf{C}}^*\delta\dot{\mathbf{v}} + \hat{\mathbf{K}}^*\delta\mathbf{v} = 0, \tag{27}$$

where $\hat{\mathbf{M}}^*$, $\hat{\mathbf{C}}^*$ and $\hat{\mathbf{K}}^*$ are the mass, the damping and the stiffness matrices of the modal equations. The mass matrix $\hat{\mathbf{M}}^*$ is given analytically in Eq. (26). The damping and the stiffness matrices may be also obtained analytically. However, a simple finite difference method is employed to obtain them in the present study. For instance, the following equation represents the simple finite difference method to calculate $\hat{\mathbf{K}}^*$:

$$\hat{\mathbf{K}}^* = \frac{\mathbf{h}(\mathbf{v}^* + \delta\mathbf{v}) - \mathbf{h}(\mathbf{v}^*)}{\delta\mathbf{v}}, \tag{28}$$

where $\mathbf{h}$ denotes $-\mathbf{R}^{\mathrm{T}}\mathbf{Q}^*$ in Eq. (26) and $\mathbf{v}^*$ represents the independent co-ordinate value in the dynamic equilibrium position.

Note that Eq. (27) is a homogeneous equation. Non-homogeneous terms are not needed to analyze the free vibration modal characteristics.

4. Numerical results and discussion

Fig. 3 shows a rotating double pendulum, which has an open kinematic loop. Two uniform bars, each of mass $m = 3$ kg and length $L = 1$ m, are connected by a pin joint. The first bar is pinned to a vertical shaft. The axes of the pin joints are parallel to each other and horizontal. If the vertical shaft is made to rotate with constant angular speed, the system can move in such a way that θ_1 and θ_2 remain constant. Therefore, $\mathbf{q}_P$ and $\mathbf{q}_R$ are chosen as follows:

$$\dot{\mathbf{q}}_P = \Omega, \tag{29}$$

$$\mathbf{q}_R = [\theta_1 \quad \theta_2]^{\mathrm{T}}. \tag{30}$$

In this system the equilibrium equations for $\mathbf{q}_R$ are given as follows:

$$\mathbf{B}_R^{\mathrm{T}}(\mathbf{M}\dot{\mathbf{B}}_P\dot{\mathbf{q}}_P - \mathbf{Q}) = 0. \tag{31}$$

These equilibrium equations can be also obtained analytically (see Ref. [15]) and these are given as follows:

$$\left(\frac{L\Omega^2}{g}\right)\cos\theta_1(8\sin\theta_1 + 3\sin\theta_2) - 9\sin\theta_1 = 0, \tag{32}$$

$$\left(\frac{L\Omega^2}{g}\right)\cos\theta_2(3\sin\theta_1 + 2\sin\theta_2) - 3\sin\theta_2 = 0. \tag{33}$$

The dynamic equilibrium positions $\mathbf{q}_R^*$ can be obtained from above equilibrium equations.

Now, the equations of motion for this system can be written as follows:

$$\mathbf{g} = \mathbf{B}_R^{\mathrm{T}}\mathbf{M}\mathbf{B}_R\ddot{\mathbf{q}}_R + \mathbf{B}_R^{\mathrm{T}}(\mathbf{M}\dot{\mathbf{B}}_R\dot{\mathbf{q}}_R + \mathbf{M}\dot{\mathbf{B}}_P\dot{\mathbf{q}}_P - \mathbf{Q}) = 0. \tag{34}$$

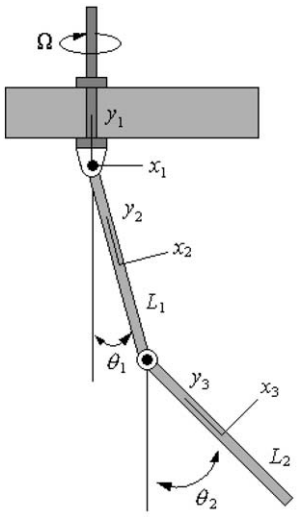

Fig. 3. Open-loop example (double pendulum).

Therefore, the linearized mass, damping, and stiffness matrices can be calculated as

$$\hat{\mathbf{M}}^* = \frac{\partial \mathbf{g}}{\partial \ddot{\mathbf{q}}_R}\Big|_{\mathbf{q}_R^*} = (\mathbf{B}_R^{\mathrm{T}}\mathbf{M}\mathbf{B}_R)_{\mathbf{q}_R=\mathbf{q}_R^*}, \tag{35}$$

$$\hat{\mathbf{C}}^* = \frac{\partial \mathbf{g}}{\partial \dot{\mathbf{q}}_R}\Big|_{\mathbf{q}_R^*} = \frac{\partial}{\partial \dot{\mathbf{q}}_R}[\mathbf{B}_R^{\mathrm{T}}(\mathbf{M}\dot{\mathbf{B}}_R\dot{\mathbf{q}}_R + \mathbf{M}\dot{\mathbf{B}}_P\dot{\mathbf{q}}_P - \mathbf{Q})]_{\mathbf{q}_R=\mathbf{q}_R^*}, \tag{36}$$

$$\hat{\mathbf{K}}^* = \frac{\partial \mathbf{g}}{\partial \mathbf{q}_R}\Big|_{\mathbf{q}_R^*} = \frac{\partial}{\partial \mathbf{q}_R}[\mathbf{B}_R^{\mathrm{T}}(\mathbf{M}\dot{\mathbf{B}}_R\dot{\mathbf{q}}_R + \mathbf{M}\dot{\mathbf{B}}_P\dot{\mathbf{q}}_P - \mathbf{Q})]_{\mathbf{q}_R=\mathbf{q}_R^*}. \tag{37}$$

The simple finite difference method is used to calculate them. The corresponding natural frequencies can be obtained analytically, too. Tables 1 and 2 show the angles of θ_1 and θ_2 in dynamic equilibrium states and the natural frequencies, respectively. The numerical results obtained by using the proposed method are in good agreement with the corresponding analytical results. Fig. 4 shows the variations of the first and the second natural frequencies. As the shaft angular speed increases, the natural frequencies decreases first and then increases. Especially, the first natural frequency reaches zero at an angular speed of the shaft before it increases. Fig. 5 shows that θ_1 and θ_2 in dynamic equilibrium states remain zero until the shaft angular speed exceeds the angular speed at which the first natural frequency becomes zero.

Fig. 6 shows a governor mechanism which has two closed kinematic loops. Body 1 of the system is the spindle which is driven by a constant angular speed; bodies 2 and 3 are pendulums which have a sphere mass at each end; and body 4 is the collar. The spindle and the pendulums are connected by revolute joints; the spindle and the collar are connected by a translational joint and a spring; and the collar and the pendulums are connected by distance joints having fixed distance of 0.1092 m. The stiffness and the free length of the spring are 1000 N/m and 0.15 m, respectively.

Table 1
Equilibrium positions of the double pendulum versus angular speed

	Analytic solution		Proposed method	
	θ_1 (rad)	θ_2 (rad)	θ_1 (rad)	θ_2 (rad)
$\omega = 3$ rad/s	0.5777	0.7404	0.5777	0.7404
$\omega = 6$ rad/s	1.347	1.405	1.347	1.405
$\omega = 9$ rad/s	1.472	1.498	1.472	1.498

Table 2
Natural frequencies of the double pendulum versus angular speed

Angular speed (rad/s)	First natural frequency		Second natural frequency	
	Present	Analytical	Present	Analytical
$\omega = 3$	1.793	1.793	7.669	7.669
$\omega = 6$	5.875	5.875	16.70	16.70
$\omega = 9$	8.963	8.963	25.19	25.19

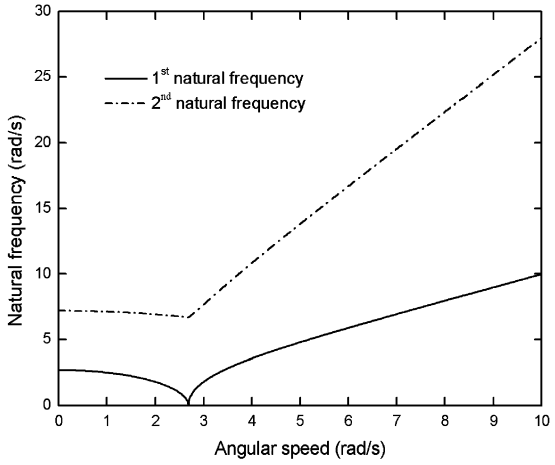

Fig. 4. Natural frequency variations versus angular speed.

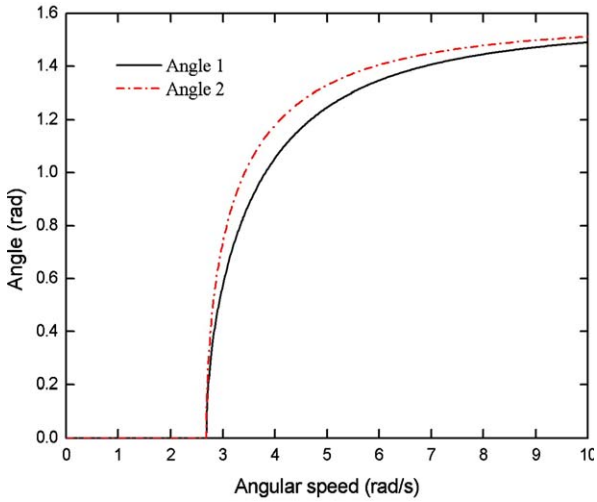

Fig. 5. Variations of the dynamic equilibrium positions.

Table 3 shows the inertia properties of the system components and Table 4 shows the coordinates of some points (shown in Fig. 6) that determine the configuration of the system. Since this system has two closed loops, two distance joints between collar and balls are cut. For modal analysis, the relative distance d between spindle and collar is chosen as an independent coordinate.

The variation of the natural frequency versus the angular speed is shown in Fig. 7. Different from the previous example, the natural frequency increases monotonically. As shown in the figure, there exists an angular speed which matches to the natural frequency. Such an angular speed is often called the critical angular speed. Since angular motion induces inertia force, the critical angular speed induces a harmonic excitation force which causes resonance of the system.

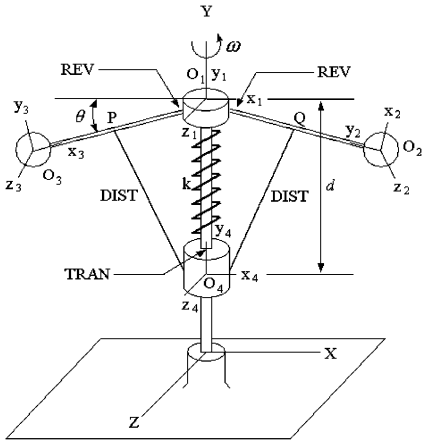

Fig. 6. Closed-loop example (governor mechanism).

Table 3
Inertia properties of the governor mechanism's bodies

Body	Mass (kg)	Moment of inertia (kg m^2)		
		$I_{x'x'}$	$I_{y'y'}$	$I_{z'z'}$
Spindle	200.0	25.0	50.0	50.0
Ball 1	1.0	0.1	0.1	0.1
Ball 2	1.0	0.1	0.1	0.1
Collar	1.0	0.15	0.15	0.15

Table 4
Initial positions of points in the governor mechanism

Point	Initial position (m)
O_1	[0.0, 0.2, 0.0]
O_2	[−0.16, 0.2, 0.0]
O_3	[0.16, 0.2, 0.0]
O_4	[0.0, 0.1256, 0.0]
P	[−0.08, 0.2, 0.0]
Q	[0.08, 0.2, 0.0]

Therefore, the operating speed of the governor mechanism needs to be located far from the critical angular speed.

Fig. 8 shows a cantilever beam which is fixed to a rotating rigid hub. The geometric and material properties of the cantilever beam are shown in Table 5. For the multibody formulation, the beam is discretized into 51 rigid bodies that are connected through 50 beam elements as shown in Fig. 8. Body 1 is the rotating hub and bodies 2–52 are the discretized rigid bodies. The hub and the ground are connected by a revolute joint; hub and body 2 are connected by a fixed joint; and the rest contiguous bodies are connected by beam elements.

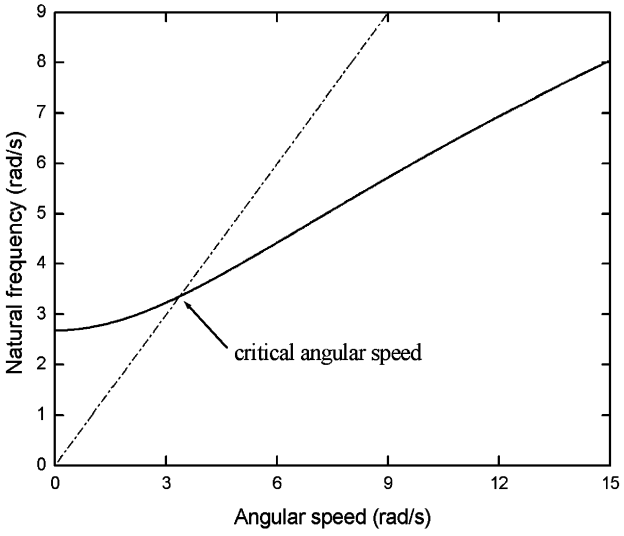

Fig. 7. Natural frequency variation versus angular speed.

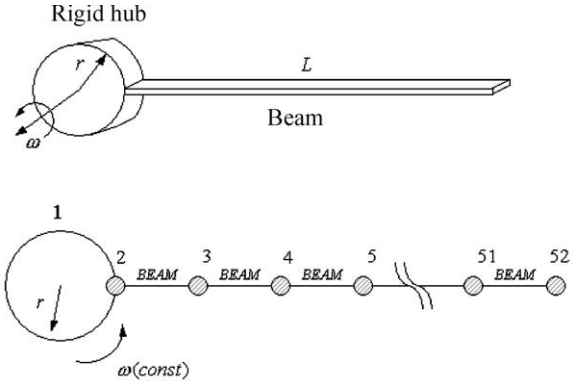

Fig. 8. Structural system example (cantilever beam).

Fig. 9 shows arbitrary two contiguous rigid bodies i and j which are connected by a beam element. In this figure, $x^i - y^i - z^i$ and $x^j - y^j - z^j$ are the body reference frame of bodies i and j, respectively; u_x^{ij}, u_y^{ij}, u_z^{ij} are relative displacements of body j with respect to body i; ϕ_x^{ij}, ϕ_y^{ij}, ϕ_z^{ij} are relative angles of body j with respect to body i; and L_0 is the initial distance between bodies i and j. The generalized forces due to the beam element can be obtained as follows:

$$\mathbf{Q}^i = \begin{bmatrix} \mathbf{A}^i \mathbf{F}_{beam} \\ \mathbf{T}_{beam} + \mathbf{A}^{i^{\mathrm{T}}} \tilde{\mathbf{d}}^{ij} \mathbf{A}^i \mathbf{F}_{beam} \end{bmatrix}, \tag{38}$$

$$\mathbf{Q}^j = \begin{bmatrix} -\mathbf{A}^i \mathbf{F}_{beam} \\ -\mathbf{A}^{j^{\mathrm{T}}} \mathbf{A}^i \mathbf{T}_{beam} \end{bmatrix}, \tag{39}$$

Table 5
Geometric and material properties of a beam

Notation	Numerical data
L (length)	6.0 m
ρ (mass per unit length)	1.2 kg/m
E (Young's modulus)	7.0E10 N/m^2
A (cross-section area)	4.0E–4 m^2
I (the area moment of inertia)	2.0E–7 m^4
r (hub radius)	0.3 m

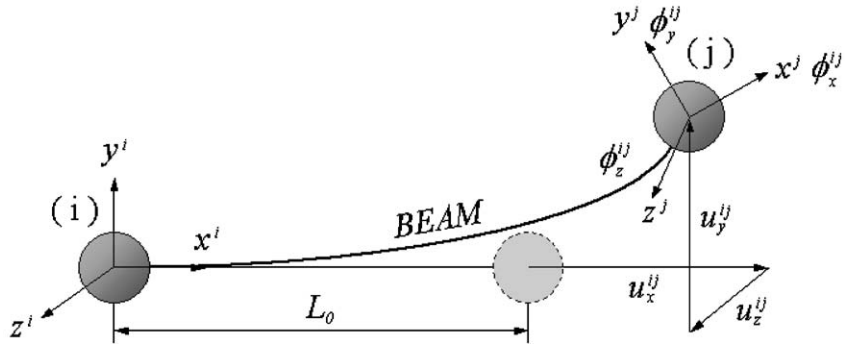

Fig. 9. Two contiguous bodies connected by a beam element.

where $\mathbf{A}^i$ and $\mathbf{A}^j$ are orientation matrices of bodies i and j, respectively and the distance vector $\mathbf{d}^{ij}$ is defined as follows:

$$\mathbf{d}^{ij} = [\mathbf{A}^i] \begin{bmatrix} L_0 + u_x^{ij} \\ u_y^{ij} \\ u_z^{ij} \end{bmatrix}. \tag{40}$$

The force and the torque due to beam can be calculated as follows:

$$\begin{bmatrix} \mathbf{F}_{beam} \\ \mathbf{T}_{beam} \end{bmatrix} = \begin{bmatrix} K_{11} & 0 & 0 & 0 & 0 & 0 \\ 0 & K_{22} & 0 & 0 & 0 & K_{26} \\ 0 & 0 & K_{33} & 0 & K_{35} & 0 \\ 0 & 0 & 0 & K_{44} & 0 & 0 \\ 0 & 0 & K_{35} & 0 & K_{55} & 0 \\ 0 & K_{26} & 0 & 0 & 0 & K_{66} \end{bmatrix} \begin{bmatrix} u_x^{ij} \\ u_y^{ij} \\ u_z^{ij} \\ \phi_x^{ij} \\ \phi_y^{ij} \\ \phi_z^{ij} \end{bmatrix}. \tag{41}$$

Table 6
Natural frequency variations versus angular speed

Angular speed (rad/s)	First frequency (rad/s)		Second frequency (rad/s)		Third frequency (rad/s)	
	Present	Ref. [17]	Present	Ref. [17]	Present	Ref. [17]
10.0	11.71	11.71	70.37	70.44	189.7	189.9
20.0	14.28	14.29	81.93	82.05	203.2	203.6
50.0	23.09	23.21	137.2	137.6	278.3	279.5
70.0	28.79	29.06	180.0	180.6	342.5	344.5
100.0	37.06	37.75	246.7	247.5	446.5	449.7

Since the Euler beam theory is used, the elements K_{ij} can be defined as follows:

$$K_{11} = EA/L, \tag{42}$$

$$K_{22} = 12EI_{zz}/L^3, \tag{43}$$

$$K_{26} = -6EI_{zz}/L^2, \tag{44}$$

$$K_{33} = 12EI_{yy}/L^3, \tag{45}$$

$$K_{35} = 6EI_{yy}/L^2, \tag{46}$$

$$K_{44} = GI_{xx}/L, \tag{47}$$

$$K_{55} = 4EI_{yy}/L, \tag{48}$$

$$K_{66} = 4EI_{zz}/L, \tag{49}$$

where E and G are Young's modulus and shear modulus of the material; I_{xx}, I_{yy}, and I_{zz} are the area moments of inertia; and L is the length of a beam. More detailed information about the beam element can be found in Ref. [16].

Table 6 shows the lowest three natural frequencies of the cantilever beam versus the angular speed of the rigid hub. The results obtained by the present multibody formulation are compared to those obtained by the method in Ref. [17]. The two results are in good agreement. The relatively small differences originate from the use of consistent mass in Ref. [17]. In Ref. [17], a non-Cartesian stretch variable along with the Rayleigh–Ritz assumed mode method is employed to derive the equations of motion. As shown in the results, the natural frequencies increase as the angular speed increases. This phenomenon is well known as the stiffening effect of the rotating beam.

5. Conclusions

In this paper, a computational algorithm is proposed to find the modal characteristics of multibody systems undergoing steady state rotational motion. Such multibody systems are often found in engineering examples. The equations of motion are derived by employing relative

co-ordinates and linearized at the dynamic equilibrium position. The mass and the stiffness matrices for the modal analysis can be obtained from the linearized equations. To verify the effectiveness and the accuracy of the proposed method, three numerical examples are solved. The results obtained by using the proposed method are compared to those obtained by analytical or previous numerical methods. It is proved that the proposed method provides accurate modal characteristics of multibody systems undergoing steady state rotational motion. The proposed method can be easily implemented into any existing multibody computer programs. Since the method does not necessitate numerical integration, it is superior to any existing methods that employ numerical integration.

Acknowledgements

This research was supported by Center of Innovative Design Optimization Technology (iDOT), Korea Science and Engineering Foundation.

References

[1] P.N. Sheth, J.J. Uicker Jr., IMP (Integrated Mechanisms Program): a computer aided design analysis system for mechanisms and linkages, *American Society of Mechanical Engineers, Journal of Engineering for Industry* 94 (1972) 454–464.
[2] N. Orlandea, M.A. Chace, D.A. Calahan, A sparsity-oriented approach to the dynamic analysis and design of mechanical systems, *American Society of Mechanical Engineers, Journal of Engineering for Industry* 99 (1977) 773–784.
[3] B. Paul, Dynamic analysis of machinery via program DYMAC, SAE Paper 770049, Warrendale, PA, 1977.
[4] E.J. Haug, R.A. Wehage, N.C. Barman, Dynamic analysis and design of constrained mechanical systems, *American Society of Mechanical Engineers, Journal of Mechanical Design* 104 (1982) 778–784.
[5] ADAMS User's Guide, MSC Software Corporation, 2003.
[6] DADS User's Manual, LMSCADSI Inc, 2002.
[7] RecurDyn User's Manual Version 4, FunctionBay Inc, 2002.
[8] V.N. Sohoni, J. Whitesell, Automatic linearization of constrained dynamical models, *American Society of Mechanical Engineers, Journal of Mechanisms, Transmissions, and Automation in Design* 108 (1986) 300–304.
[9] A.G. Lynch, M.J. Vanderploeg, A symbolic formulation for linearization of multibody equation of motion, *American Society of Mechanical Engineers, Journal of Mechanical Design* 117 (1995) 441–445.
[10] D.S. Bae, E.J. Haug, A recursive formulation for constrained mechanical system dynamics: Part I. Open loop systems, *Mechanics of Structures and Machines* 15 (3) (1987) 359–382.
[11] D.S. Bae, E.J. Haug, A recursive formulation for constrained mechanical system dynamics: Part II. Closed loop systems, *Mechanics of Structures and Machines* 15 (4) (1987) 481–506.
[12] P.E. Nikravesh, *Computer-Aided Analysis of Mechanical Systems*, Prentice-Hall, Englewood Cliffs, NJ, 1988.
[13] S.S. Kim, M.J. Vanderploeg, A general and efficient method for dynamic analysis of mechanical systems using velocity transformations, *American Society of Mechanical Engineers, Journal of Mechanisms, Transmissions and Automation in Design* 108 (1986) 176–182.
[14] R.M. Rosenberg, *Analytical Dynamics of Discrete Systems*, Plenum Press, New York, 1977.
[15] T.R. Kane, D.A. Levinson, *Dynamics: Theory and Applications*, McGraw-Hill, New York, 1985.
[16] J.S. Przemieniecki, *Theory of Matrix Structural Analysis*, McGraw-Hill, New York, 1968.
[17] H.H. Yoo, S.H. Shin, Vibration analysis of rotating cantilever beams, *Journal of Sound and Vibration* 212 (5) (1998) 807–828.